

HUMAN IRON REGULATORY PROTEIN 2 IS EASILY CLEAVED IN ITS SPECIFIC DOMAIN: CONSEQUENCES FOR THE HEME BINDING PROPERTIES OF THE PROTEIN.

Camille DYCKE ^{*†‡¹}, Catherine BOUGAULT^{‡§¶}, Jacques GAILLARD[£], Jean-Pierre ANDRIEU^{‡¶¥}, Kostas PANTOPOULOS^{|^μ}, Jean-Marc MOULIS^{*†‡}

* CEA, DSV, IRTSV, Laboratoire de Chimie et Biologie des Métaux, 17 rue des Martyrs, Grenoble, F-38054, France.

† LCBM, CNRS, Grenoble, France.

‡ Université Joseph Fourier, Grenoble, France.

§ Institut de Biologie Structurale- Jean-Pierre Ebel, Laboratoire de Résonance Magnétique Nucléaire, 41 rue Jules Horowitz, F-38027 Grenoble, France.

¶ IBS, CNRS, Grenoble, France.

£ Département de Recherche Fondamentale sur la Matière Condensée, Service de Chimie Inorganique et Biologique; 17 rue des Martyrs, Grenoble, F-38054, France.

¥ Institut de Biologie Structurale- Jean-Pierre Ebel, Laboratoire d'Enzymologie Moléculaire, 41 rue Jules Horowitz, F-38027 Grenoble, France.

| Lady Davis Institute for Medical Research, 3999 Côte Ste Catherine, H3T 1E2, Montréal, Québec, Canada.

^μ Department of Medicine, McGill University, Montréal, Québec, Canada.

Short title: cleavage of Iron Regulatory Protein 2 and heme-binding

Correspondence: J-M. Moulis, CEA-Grenoble, IRSTV/LCBM, 17 rue des Martyrs, 38054 Grenoble Cedex 9, France. Tel. 0033438785623; e-mail: jean-marc.moulis@cea.fr

¹ present address: Covance Laboratories Limited, Otley Road, Harrogate, North Yorkshire, HG3 1PY UK

ABSTRACT

Mammalian Iron Regulatory Proteins, IRP1 and IRP2, are cytosolic RNA-binding proteins that post-transcriptionally control the mRNA of proteins involved in storage, transport, and utilization of iron. In iron-replete cells, IRP2 undergoes degradation by the ubiquitin/proteasome pathway. Binding of heme to a 73 amino acids domain (73aa-Domain) that is unique in IRP2 has been previously proposed as the initial iron-sensing mechanism. It is shown here that recombinant IRP2 and the 73aa-Domain are sensitive to proteolysis at the same site. Nuclear Magnetic Resonance data suggest that the isolated 73aa-Domain is not structured. Iron-independent cleavage of IRP2 within the 73aa-Domain also occurs in lung cancer (H1299) cells. Heme interacts with a cysteine residue only in truncated forms of the 73aa-Domain, as shown by a series of complementary physico-chemical approaches, including Nuclear Magnetic Resonance, Electron Paramagnetic Resonance, and ultra-violet visible absorption spectroscopy. In contrast, the cofactor is not ligated by the same residue in the full-length peptide or intact IRP2, although non specific interaction occurs between these molecular forms and heme. Therefore it is unlikely that the iron-dependent degradation of IRP2 is mediated by heme binding to the intact 73aa-Domain, since the sequence resembling a Heme Regulatory Motif in the 73aa-Domain does not provide an axial ligand of the cofactor unless this domain is cleaved.

Key words: iron, heme, NMR, proteolysis, regulatory motif.

Abbreviations used: 73aa-Domain, DMEM, Dulbecco's modified Eagle medium; DTT, dithiothreitol; EDAC, 1-ethyl-3-(3-dimethylaminopropyl)carbodiimide; HA, hemagglutinin; IRP2 peptide encoded by exon 5; HRM, Heme Regulatory Motif; IRE, Iron Responsive Element; IRP, Iron Regulatory Protein(s); PBS, phosphate-buffered saline; PMSF, phenylmethanesulphonylfluoride.

INTRODUCTION

Iron Regulatory Proteins (IRP) are ubiquitous regulators of cellular iron homeostasis. They are cytosolic RNA-binding proteins that post-transcriptionally control translation of proteins involved in storage (ferritin), transport (e.g. transferrin receptor 1), and use (e.g. erythroid α -aminolevulinic acid synthase) of iron. The two metazoan IRP, IRP1 and IRP2, bind with high affinity to RNA stem-loop structures known as iron-responsive elements (IRE) located in the 3' or in the 5'-untranslated regions of mRNA. Depending on the 3' or 5' position of IRE with respect to the coding sequence, the binding of IRP induces mRNA stabilization or translational inhibition, respectively [1]. The relative importance of this regulatory system may change under different conditions and for different cell types [2]. For instance, IRP play a prominent role in adjusting protoporphyrin synthesis to transferrin-bound iron availability in erythroblasts as suggested by the zebrafish anemia induced by sustained activation of IRP1 [3]. But synthesis of proteins participating in iron homeostasis does not always fit with the IRE-IRP model of regulation along differentiation of the lineage [4, 5]. Other regulatory events, including transcriptional ones, may combine with, or supersede, the translational control carried out by IRP.

Therefore, the precise role of the IRP-IRE system in mammalian iron homeostasis has received a lot of attention over the last few years after knockout animals were generated. IRP2^{-/-} mice develop microcytic anemia [6-8], whereas IRP1^{-/-} mice are asymptomatic. Inactivation of both IRP1 and IRP2 is lethal at an early stage during embryonic development [9]. The disruption of IRP2 has also been associated with brain iron overload and the development of a neurodegenerative movement disorder [6, 9]. However, other IRP2^{-/-} mice do not show obvious signs of neurodegeneration [10]. Thus, despite these significant progresses, the respective roles of IRP1 and IRP2 in cellular iron homeostasis remain to be fully delineated. However IRP2 is often proposed to be the main regulator under normal conditions, since IRP1 is mainly under a non-IRE binding form in tissues, and it does not seem to be able to always replace IRP2 in animals deficient for the gene of the latter protein [11, 12].

The cellular concentration of IRP2 results from the equilibrium between *de novo* synthesis and degradation [13]. In iron-replete cells, IRP2 is rapidly degraded by the ubiquitin/proteasome pathway [14, 15]. Early work led to the conclusion that a proline and cysteine-rich stretch of 73 amino acids (73aa-Domain) encoded by the unique IRP2-specific exon 5 is necessary and

sufficient for IRP2 degradation by a mechanism involving oxidation of cysteines upon iron binding and polyubiquitination [14, 16]. More recent results have proposed that the 73aa-Domain plays a role in IRP2 degradation in response to heme, and that the cysteine residue of a Cys-Pro-Phe-His, Heme Regulatory-like, motif in the domain binds oxidized heme [17-19]. However, studies by independent groups showed that an IRP2 deletion mutant lacking the full-length domain remains sensitive to iron-dependent degradation, similar to wild type IRP2 [20, 21].

To get direct information about the role of the 73aa-Domain in IRP2 degradation, the recombinant protein and the 73aa-Domain were purified and their interaction with heme was studied with a series of complementary methods. We have discovered a highly susceptible proteolytic site in IRP2-specific 73aa-Domain. Such cleavage site may have remained undetected in previous studies and it strongly influences the heme-binding properties of the protein. Its widespread occurrence, both *in vitro* and inside cells, may explain at least part of the previous conflicting results obtained with IRP2.

EXPERIMENTAL

Plasmids

IRP2 cDNA was extracted from the pET16b-IRP2 plasmid constructed at EMBL-Heidelberg. *NdeI* and *ClaI* sites were used to subclone the IRP2 cDNA into the pT7-7 bacterial expression plasmid [22] to give pTIRP2.

The DNA fragment encoding the 73 amino acids domain (73aa-Domain), corresponding to exon 5 of the hIRP2 gene, was obtained by PCR amplification with the 5'-GACTTCAGCATATGGCAATACAGAATGCACC-3' (forward) and 5'-CTTGATTTTACACGAATTCTCATTCAGGCACTGG-3' (reverse) primers from the above pTIRP2 plasmid. The fragment was digested with *NdeI* and *EcoRI*, and cloned into the pTYB12 plasmid (IMPACT System, New England Biolabs, Inc, Beverly, MA, USA) to give pTYB12/73-D. This plasmid encodes the 73aa-Domain sequence N-terminally fused to the intein gene. The correct construction of pTYB12/73-D was checked by sequencing.

73aa-Domain production in *E.coli*

Plasmid pTYB12/73-D was used to transform ER2566 competent cells (F⁻ λ⁻ *fhuA2* [*lon*] *ompT* *lacZ*::T7 *gene1* *gal* *sulA11* Δ(*mcrC-mrr*)114::IS10 *R*(*mcr-73::miniTn10-TetS*)2 *R*(*zgb-*

210::Tn10)(*TetS*) *endA1* [*dcm*] from New England Biolabs) and grown in Luria Broth medium (Gibco BRL, Paisley, UK) supplemented with 100 µg/ml ampicillin at 37°C until early log-phase. Induction was carried out for 4 hr at 22°C after addition of 0.5 mM isopropyl β-D-1-thiogalactopyranoside (IPTG).

73aa-Domain purification

Cells were harvested at 5000 *g* for 30 min at 10°C and the cell pellet was suspended in 50 mM potassium phosphate buffer pH 8 with 250 mM NaCl (buffer A). Oxygen was removed from the gas phase by bubbling purified argon. Cell suspensions were broken by sonication and centrifuged 30 min at 20 000 *g* and 4°C. The supernatant was loaded anaerobically on a chitin beads column (New England Biolabs) equilibrated with buffer A for affinity chromatography. After two washes with the same buffer, cleavage of the fused intein-73aa-Domain protein was carried out on the column with 3 volumes of the same buffer adjusted at pH 7.2 and containing 50 mM of dithiothreitol (DTT). The resin was left either at room temperature for 40 hr or at 4°C in the presence of 5 µM phenylmethanesulphonylfluoride (PMSF), depending on the experiment (see Results). Excess buffer was removed to elute the 73aa-Domain fragment and the column was washed with 3 volumes of buffer A. Eluted fractions were analyzed by SDS-PAGE on a 15% acrylamide gel. Fractions containing the expected peptide of ca. 8 kDa were pooled and concentrated on a YM3 membrane (3000 Da cut off value, Amicon Millipore, Danvers, MA, USA). The concentrated fraction was further purified by gel filtration through a BioGel P10 (BioRad, Hercules, CA, USA) column equilibrated with 50 mM potassium phosphate buffer at pH 6.2 containing 250 mM NaCl. A single protein fraction was eluted and the purification yield was 1.3 mg/l culture.

IRP2 production in *E.coli*

The pTIRP2 plasmid was used to transform K38 cells already containing the pGP1-2 plasmid [22]. The latter plasmid bears the T7 RNA polymerase gene under the control of the λp_L promoter, and the cI-857 temperature-sensitive repressor. Cells were grown in Terrific Broth (Gibco BRL, Paisley, UK) with 100 µg/ml ampicillin and 50 µg/ml kanamycin at 30°C for 20 hr. Induction was carried out by increasing the temperature to 42°C for 1 hr 30 min, prior to production at 30°C for 6 hr.

IRP2 purification

All purification steps were carried out under argon to avoid uncontrolled protein oxidation. IRP2 was monitored by electrophoretic mobility shift assays to detect IRP2 RNA-binding activity [23]. Cells were harvested at 4000 *g* and 25°C for 30 min: the cell pellet was resuspended in 20 mM Tris-Cl, 5 μ M PMSF, pH 7.4 and frozen. After thawing, lysates were prepared by sonication and centrifuged at 45 000 *g* and 20°C for 1 hr. Ammonium sulfate (1.07 M, 30% saturation at 4°C) was added to the supernatant prior to 30 min centrifugation at 12 000 *g* and 4°C. The resulting supernatant was brought to 3.2 M ammonium sulfate (60% saturation) and centrifuged 90 min at 12 000 *g* and 4°C. The pellet was resuspended in 20 mM Tris-Cl, 5 μ M PMSF, 1% (v:v) glycerol, pH 8 and dialyzed for 2 hr against the same buffer, followed by overnight dialysis against this buffer supplemented with 0.1 mM DTT. The dialyzed supernatant was centrifuged 30 min at 45 000 *g* and 20°C before being loaded on a 50-ml diethylaminoethyl cellulose column (DE52 Whatman International Ltd Maidstone, UK) equilibrated with dialysis buffer. Elution was carried out with a discontinuous gradient of sodium chloride in the same buffer: two column volumes of 0.15 M NaCl were followed by 3 column volumes of 0.3 M NaCl. Ammonium sulfate (0.4 M) was added to the eluted active fractions, followed by centrifugation for 20 min at 18 000 *g* and 20°C. The supernatant was loaded on a 200 ml-Phenyl Sepharose 6B column (GE Healthcare, Orsay, France) equilibrated with 20 mM Tris-Cl, 5 μ M PMSF, 1% Glycerol, 0.1 mM DTT, 0.4 M (NH₄)₂SO₄, pH 8. Elution was carried out by decreasing the ammonium sulfate concentration in the same buffer. The active fraction was desalted by overnight dialysis and loaded and filtrated on a 2L-Superdex 200 column (GE Healthcare, Orsay, France) equilibrated with 50 mM Tris-Cl, 1% Glycerol, 0.1 mM DTT, 50 mM NaCl, pH 8. The active fraction was loaded on 50 ml of hydroxyapatite (Bio-Gel Hydroxyapatite HTP, Bio-Rad, Hercules, CA, USA) equilibrated with 20 mM Tris-Cl, 1% Glycerol, 0.1 mM DTT, pH 7.4. Elution was carried out using increasing potassium phosphate concentrations between 5 and 200 mM with 1% glycerol and 0.1 mM DTT. The last step of IRP2 purification involved HPLC heparin-affinity (GE Healthcare Orsay, France) by applying a gradient of potassium chloride in 20 mM Hepes-OH, 0.1 mM DTT, pH 7.4.

Heme-agarose affinity gel resin synthesis

Two ml of Affi-Gel 102 cross-linked agarose (Biorad, Hercules, CA, USA) suspension were washed twice with water, twice with dimethylformamide (DMF) and resuspended in DMF. Ten

mg of hemin chloride (Sigma Aldrich France, Saint-Quentin Fallavier) were dissolved in 3 ml DMF and added to the gel. EDAC (1-ethyl-3-(3-dimethylaminopropyl)carbodiimide) was used as coupling reagent for carboxyl-containing ligands. Three hundred mg EDAC were dissolved in 800 μ l of 50% DMF in water. One hundred μ l of the EDAC solution was added to the heme-agarose mixture before acidification with 1M HCl to pH 3. A further 400 μ l of EDAC were added before re-acidification to pH 4. The mixture was left to react for 3 hr at room temperature on a rotating rod and the pH was adjusted every 30 min. A last 700 μ l of the EDAC solution were added to the reaction mixture and left rotating overnight. After 21 hr the reaction was stopped by adding 300 μ l of 1 M NaOH to increase the pH to 7.5. The heme-linked resin was washed 3 times in DMF. The supernatant was colorless on the final rinse and the resin had a pale brown color indicating the presence of heme. The resin was resuspended in 1.5 ml of 0.1 M NaCl.

Coupling efficiency was calculated indirectly. Unreacted heme recovered in the resin washes was quantitated using spectrophotometry and subtracted from heme added to the initial reaction mixture. Forty two μ l of recovered supernatant from resin washes was diluted 100 times in water. One ml pyridine was added followed by 0.5 ml of 1 M NaOH. Five mg of sodium dithionite were added and absorbance of this solution was measured at 419 nm. Coupling yield was 1.5 μ mol heme / ml agarose resin.

Interaction between heme-agarose resin and purified proteins

The heme bound resin was washed twice with water, twice with 8 M urea and twice with elution buffer (50 mM sodium phosphate, 0.5 M NaCl, pH 7.3) prior to incubation with purified proteins. To check for the trapping efficiency of the resin toward apo-heme proteins, 50 μ l of resin, resuspended in elution buffer, were incubated for 2 hours on a rotating rod with 20 μ g purified apomyoglobin. The same amount of apomyoglobin was also incubated with 50 μ l of non-derivatized Affi-Gel as a control of binding specificity. The same procedure was applied to 5 μ g of purified IRP2 with 30 μ l of resin under identical conditions. Unbound proteins were first eliminated in the supernatant of a 2 minute-, 10000 *g*-centrifugation, then by washing the resin with 50 mM sodium phosphate, 0.5 M NaCl, pH 7.3. Bound proteins were eluted after thorough mixing with 8 M urea in the same buffer for 10 min. Protein fractions were precipitated using 10% trichloroacetic acid and resuspended in sample buffer (10% 2-mercaptoethanol, 6% SDS, 20% glycerol, 0.2 mg/ml bromophenol blue) before being denaturated and analyzed by SDS-PAGE and Western blot.

Culture of the H1299 lung cancer cell line

H1299 lung cancer cells were maintained in Dulbecco's modified Eagle medium (DMEM) supplemented with 10% fetal bovine serum, 2 mM glutamine, 100 U of penicillin/ml, and 0.1 mg of streptomycin/ml. The clones producing HA-tagged wild type human IRP2 or hemagglutinin (HA)-tagged IRP2 with deletion of the specific 73 amino acids domain, IRP2 Δ 73, under the control of a tetracycline-inducible promoter were maintained in DMEM containing 2 μ g of tetracycline/ml, 2 μ g of puromycin/ml and 250 μ g of G418/ml. H1299 cells were plated for 48 hr in tetracycline-free media to express IRP2-HA or IRP2 Δ 73-HA cDNA. Tetracycline (2 μ g/ml) was then added back to shut off transcription. No protease inhibitors were added to the culture medium.

Plasmids expressing the IRP2-HA and IRP2 Δ 73-HA cDNA were prepared and transfected in H1299 lung cancer cells as described elsewhere [21, 24].

Proteins extraction from the H1299 lung cancer cell line

H1299 cells were harvested and washed twice with phosphate-buffered saline (PBS). Cell pellets were resuspended in lysis buffer (1% Triton X-100, 25 mM Tris-Cl, pH 7.4, 40 mM KCl) in the presence of protease inhibitors (a mixture of (aminoethyl)benzenesulfonyl fluoride, pepstatin A, L-trans-epoxysuccinyl-leucyl amido(4-guanidino)butane, bestatin, leupeptin and aprotinin, Sigma) and incubated 20 min in ice prior to 15 min centrifugation at 4°C and 15000g. Total protein concentrations were determined with the Bio-Rad (Bio-Rad Laboratories GmbH, Muenchen, Germany) protein assay.

Western blotting

Fifty μ g of total proteins were resolved by SDS-PAGE on 8% gels, and proteins were transferred to nitrocellulose membranes. The blots were saturated with 10% non-fat milk in PBS-Tween 0.2% and probed overnight at 4°C with antibodies against HA (Santa Cruz Biotechnologies Inc, Santa Cruz, California, USA) or β -actin (Sigma) at dilutions 1:1000 in PBS-Tween 0.2% with 5% non-fat milk. To directly probe IRP2, antibodies against the QKAGKLSPLKVQPKKL peptide (amino acids 151 to 167) of human IRP2 (a kind gift from Dr Cécile Bouton, ICSN, Gif-sur-Yvette, France) were used at 1:2000 dilution. Following three washes with PBS-Tween 0.2%, the blots were incubated with peroxidase-coupled goat anti-rabbit immunoglobulin G at dilution 1:5000 for 2 hr at room temperature, before detection by the enhanced chemiluminescence

method (ECL, GE Healthcare Orsay, France). Alternatively the blots were incubated for 2 hr with alkaline phosphatase-coupled goat anti-rabbit immunoglobulin G at dilution 1:5000 at room temperature, followed by colorimetric detection (Sigma Fast BCIP/NBT). The results shown in the Figures are representative of several independent experiments.

NMR analysis

Peptide samples were prepared for NMR in 50 mM phosphate buffer, 250 mM NaCl, pH 6.2 in H₂O:D₂O 90:10 under anaerobic conditions at concentrations ranging from 200 μM to 300 μM. NMR tubes were generally sealed with gas-tight caps, unless otherwise indicated.

¹H NMR spectra were recorded at 25°C on a Varian Inova 600 spectrometer equipped with a penta ¹H/³¹P/¹³C/²H/¹⁵N resonance probe operating at 600 MHz on the proton channel. Water suppression on a 10 ppm spectral width was achieved using a classical watergate sequence [25] after optimization of water-selective gaussian pulses. A 2.5 s-recycle delay was used to collect these data. During processing, residual water was further suppressed using a frequency filter and truncation artefacts were removed using a standard gaussian window function over the 6913 Hz spectral width. Chemical shifts were externally referenced to 2,2-dimethyl-2-silapentane- 5-sulfonate sodium salt at 25°C. To improve sensitivity, 2D ¹H,¹H-spectra were collected at 25°C on a Varian Inova 800 spectrometer equipped with a triple ¹H/¹³C/¹⁵N resonance cold probe operating at 800 MHz on the proton channel. Nuclear Overhauser Effect Spectroscopy (NOESY) and Total Correlation Spectroscopy (TOCSY) spectra were recorded with 150 ms and 70 ms mixing times, respectively, using sculpting for water suppression [26] and a 1.1 s relaxation delay. Efficient water suppression was detrimental to the detection of backbone amide protons exchanging with water, but beneficial for the detection of aromatic residues such as phenylalanines. A HET-SOFAST ¹H spectrum was also collected with acquisition parameters suitable to assess peptide compactness [27].

Other methods

Absorption spectra, Electron Paramagnetic Resonance spectra [28], and N-terminal sequencing [29] were obtained as previously described.

RESULTS

The purified 73 amino acids domain of IRP2 is susceptible to proteolysis

The 73aa-Domain of IRP2 was produced in *E.coli* using the intein-tag system and purified after on-column cleavage under reducing conditions (see Experimental). The final fraction was loaded on a 15% acrylamide gel and analyzed by Western blot using antibodies raised against IRP2. Fast migrating immunoreactive material was detected, as expected for the 73aa-Domain of IRP2 (not shown). However, analysis by N-terminal Edman sequencing gave several sequences, corresponding to 4 truncated forms of the 73aa-Domain (Figure 1A). Proteolysis occurred near closely spaced lysine residues, resulting in truncated peptides of ca. 45 amino acids (and a minor one of 51), containing the C-terminus of the 73aa-Domain and encompassing all cysteines encoded by IRP2 exon 5. In the following this C-terminal part of the peptide with heterogeneous N-termini will be called the 'truncated peptide'.

In order to reduce proteolysis, a similar purification procedure was carried out at low temperature by minimizing proteolytic activities. N-terminal sequencing revealed the presence of one major sequence starting at the expected intein cleavage site, indicating purification of full-length IRP2 73aa-Domain.

These results indicate that IRP2 73aa-Domain is highly sensitive to proteolytic cleavage, but that proteolysis in bacterial lysates can be largely avoided by adding the serine protease inhibitor PMSF during the purification steps. Therefore, PMSF was added in all samples obtained by breaking cells, except in the experiments aiming at isolating cleaved proteins or peptides.

Recombinant IRP2 is also efficiently cleaved at the same site

It was of interest to know whether the 73aa-Domain cleavage was limited to the isolated peptide or if the same site in the complete IRP2 protein was also prone to proteolysis. Following expression in *E.coli* and purification, the final fraction of human IRP2 was active (Figure 1B) and it was analyzed by electrophoresis (Figure 1C). Two major bands of ~106 and ~80 kDa were detected and subjected to N-terminal Edman sequencing. The 106 kDa band was found to be the full-length purified IRP2, whereas the N-terminus of the 80 kDa band was a mixture of two sequences beginning with Lys-Val-Gln-Pro-Lys-Lys-Leu-Pro- and Lys-Leu-Pro-Cys-Arg-Gly-Gln-Thr. In agreement with the data of Figure 1A, these fragments correspond to cleavage sites

located in the 73aa-Domain. They indicate that two truncated forms are significantly produced from recombinant IRP2, despite the addition of PMSF during the purification steps. These results show that the 73aa-Domain is particularly susceptible to proteolysis in the whole molecule and indicate that this region is probably highly accessible, as predicted from the 3D structure of the homologous IRP1 protein [30].

Thus, analysis of the degradation products of both purified 73aa-Domain and IRP2 points to the specific susceptibility of this domain to proteolytic cleavage.

Proteolytic cleavage of IRP2 occurs in H1299 cells producing IRP2-HA

The cleavage sites in the 73aa-Domain of IRP2 were evidenced above with purified proteins. To address whether cellular IRP2 is also sensitive to cleavage at the same sites, H1299 lung cancer cells producing HA-tagged IRP2 (IRP2-HA) or a version devoid of the 73aa-Domain (IRP2_{Δ73}-HA) were studied.

The cells were plated for 48 hr in tetracycline-free media to accumulate IRP2-HA. Tetracycline was then added to shut off IRP2-HA synthesis and IRP2-HA levels were monitored at different time intervals by Western blot with HA antibodies. A second band of ca. 80 kDa was clearly detected in addition to the 106 kDa band corresponding to full-length IRP2 (Figure 2A). The ca. 80 kDa size matches that of the truncated recombinant IRP2 determined *in vitro*. The intensity of the 80 kDa band changed in parallel with the major 106 kDa band in all experiments, indicating that the amount of the 80 kDa band was related to that of IRP2. Beyond 8 hr after stopping IRP2 production, the protein concentration was largely decreased and the 80 kDa band became undetectable, indicating further degradation.

In order to establish whether proteolysis occurred before or after cell lysis, the experiments were carried out either in the presence or in the absence of proteases inhibitors during the preparation of extracts (see Experimental). Similar results to those shown in Figure 2A were obtained by Western blot analysis under both sets of experimental conditions, indicating that IRP2-HA proteolysis was probably not occurring upon sample processing after cell lysis.

We next examined whether iron had some effect on the 80 kDa cleavage product. After induction of IRP2 for 48 hr, tetracycline was added back and 50 µg/ml ferric ammonium citrate or 100 µM of the iron chelator desferrioxamine were added after one hour. Seven hours later the cells were lysed and the band at 80 kDa was detectable in Western blots under all conditions in

proportion of the IRP2 amount (Figure 2B). Therefore, the specific cleavage of IRP2 was not sensitive to these treatments.

To further assess whether the cleavage site evidenced *in vitro* (Figure 1) is responsible for the appearance of the truncated form of IRP2 in cells, the same experiments were carried out with H1299 cells producing HA-tagged IRP2 $_{\Delta 73}$ in which the 73aa-Domain is absent (Figure 2C). Up to 8 hr after the end of the induction period, a band of 98 kDa corresponding to intact IRP2 $_{\Delta 73}$ was observed. No smaller bands were detected, suggesting that degradation of IRP2 $_{\Delta 73}$ does not generate sufficiently stable intermediates that can be detected on these gels. Comparison of Figures 2A and 2C indicates that the IRP2 specific cleavage occurs in the 73aa-Domain.

It has been established that iron accelerates IRP2 degradation [14, 31] and it has been proposed that IRP2 detects intracellular iron levels by binding heme via the 73aa-Domain [17-19] in a process triggering its degradation [19, 32]. Since the cleavage sites shown in Figure 1A leave truncated fragments containing all four cysteines and the histidine of the 73aa-Domain, but none of the lysines, it was of interest to investigate heme and metal binding to these peptides.

^1H -NMR does not evidence folding of either truncated or full-length 73aa-Domain, even in the presence of iron or heme

Purification of the 73aa-Domain was carried out under argon and in the presence of dithiothreitol to avoid oxidative damage to the peptide. The starting material of the following experiments is thus the reduced peptide in which cysteines occur as free thiol groups. These experiments were carried out in relatively dilute solutions, 300 μM at most, since purified 73aa-Domain precipitates at higher concentrations. The ^1H -watergate spectrum of the truncated peptide is reported in Figure 3A. In what follows, 'truncated peptide' refers to the mixture of cleaved peptides identified in Figure 1A. All of the detected signals fall into the 0.8 to 8.6 ppm range. A narrow and intense signal centered around 1 ppm accounts for the methyl groups of the molecule, and the spectra display a particularly low ratio of protons in the amide/aromatic region between 6 and 9 ppm as compared to the aliphatic region. These features are indicative of the absence of secondary and tertiary structure elements in the peptide. This is further confirmed by the absence of any inter-residue correlation in an extended series of NOESY (and ROESY) experiments, as well as by a 0.80 λ_{noe} value in the 1D-HET $^{\text{noe}}$ -SOFAS NMR spectrum [27] collected at 800

MHz (data not shown). These results strongly suggest that the truncated peptide of the 73aa-Domain does not fold under these experimental conditions.

Qualitatively similar results were obtained with full-length 73aa-Domain (Figure 3B): the region spanned by the ^1H -NMR signals is as narrow as in the case of the truncated peptide, and no inter-residue NOE were detected. Therefore, the full-length peptide does not display secondary structure elements and the additional presence of the lysine- and proline-rich N-terminal sequence of the 73aa-Domain (Figure 1A) does not help folding of this domain. Furthermore, the ^1H -watergate spectrum in Figure 3B reveals a hump below sharp resonances in the aromatic/amide region suggesting that the full-length peptide has a tendency to aggregate or to sample a series of different conformations in solution at the concentrations used for the NMR study.

The truncated peptide was then oxidized either by bubbling oxygen into the sample or by addition of an excess of ferricyanide. Neither of these treatments did significantly change the initially recorded ^1H -NMR spectrum of the truncated peptide (data not shown). Therefore, oxidation of the truncated domain did not favor peptide folding, or the ^1H -NMR spectra of the folded fraction, if any, escaped detection under these experimental conditions.

If the 73aa-Domain acts as a sensor, addition of metals may contribute to some conformational changes and folding. Addition of zinc chloride did not induce any major changes in the ^1H -watergate spectrum of the full-length (data not shown) or the truncated peptide (Figure 3C). The ^1H -spectra of the truncated peptide (Figure 3A) show displacement of amide proton resonances from the 8 – 8.5 ppm range to the 7.5 – 8 ppm region, as well as broadening of some resonances, in the presence of ferrous iron (Figure 3D). These small effects are assigned to the paramagnetism of Fe(II) ions at room temperature and local perturbations arising from slight pH changes or non specific iron-binding. Despite these minor changes, divalent cations, including Fe(II), do not induce folding of the two studied forms of the 73aa-Domain.

Next, reduced truncated 73aa-Domain was incubated with excess of hemin and gel-filtrated to remove unbound cofactor. The filtrated protein fraction was colored, indicating that some heme-containing compound co-eluted. However, no major changes, such as extensive signals spreading or overall significant signal intensity alteration, were observed in the ^1H -watergate spectra (compare Figure 3A and 3E). The same experiment carried out with full-length 73aa-Domain gave qualitatively similar results (see Figure 3B and 3F).

Conformations of truncated or full-length 73aa-Domain studied by TOCSY

The information content of 1D-NMR is nevertheless scanty and the 73aa-Domain samples at their low solubility limits are not likely to display strong NOE. Therefore these samples were compared by a NMR method circumventing part of these problems, namely by recording TOCSY spectra. Since hemin-reacted and gel-filtrated full-length 73aa-Domain samples retained the color of the cofactor, some interaction must occur. Indeed, TOCSY spectra of such samples displayed slightly less off-diagonal signals in the amide and aliphatic regions than spectra of the same peptide without hemin, although most of the spin-systems were clearly conserved between the two samples. In contrast, only signals of 2 spin-systems, that were not present in spectra of the 73aa-Domain without heme, were observed in the spectra of the hemin-reacted material (Table 3 of Supplementary Data). These data are not in favor of a clear, strong, and specific binding of hemin to the full-length 73aa-Domain peptide, an event that should change a subset of spin systems corresponding to residues in the vicinity of the binding site.

Comparison was then made between truncated and full-length peptides. The number of off-diagonal signals over the full range TOCSY spectra of hemin-reacted truncated 73aa-Domain was not significantly smaller than that detected with the corresponding full-length sample (data shown for only part of the aromatic region in Figure 4). Only a few correlations in the full-length peptide, such as those annotated b_4 - b_6 in Figure 4B, were absent in truncated 73aa-Domain spectra (Figure 4A). However, many spin systems were clearly shifted between these two samples. In most cases, the signals could not be sequence-specifically assigned because the 73aa-Domain contains many occurrences of the same amino acids. One important exception is for phenylalanines: the 73aa-Domain sequence has two phenylalanine residues in its C-terminal part, so that both are present in truncated 73aa-Domain. The two phenylalanine side-chain proton signals can be identified in the TOCSY spectra of the truncated (Figure 4A, inserts A1 and A2) and full-length (Figure 4B, inserts B1 and B2) peptides. Both phenylalanine rings appear as intense and narrow signals, in the truncated peptide with spectroscopic signatures a_{1i} and a_{2i} (Figure 4A, inserts A1 and A2, Figure 4C) and in the full-length peptide with spectroscopic signatures b_{1i} and b_{2i} (Figure 4B, inserts B1 and B2, Figure 4D). Detailed analysis of these phenylalanine signals can be found as Supplementary Data. It indicates that heme interaction perturbs the NMR signatures of these residues in different ways for the two forms of the 73aa-Domain.

Furthermore, some of the TOCSY signals that were found to shift or disappear upon association of hemin with full-length 73aa-Domain were recovered for truncated 73aa-Domain in the presence of hemin (Table 1 of Supplementary Data). One likely explanation for these data is that hemin interaction with full-length 73aa-Domain occurs through non-specific association of the high-spin ferric cofactor with the peptide, in agreement with other spectroscopic data (see below). As a result, the relaxation properties of the signals for protons close enough to heme change, and the corresponding signature becomes invisible in conventional TOCSY experiments. In the case of truncated 73aa-Domain, hemin mainly binds to a specific site and paramagnetic relaxation does not perturb the same signals. Therefore, the signals lost in hemin-reacted full-length 73aa-Domain are recovered in hemin-reacted truncated 73aa-Domain as they occurred for the peptide in the absence of heme. Support for this interpretation is provided in the following, by implementation of complementary methods.

Additional spectroscopic evidence for interaction between heme and the truncated peptide

In order to further characterize the interaction between heme and the 73aa-Domain, absorption spectra were recorded. The absorption spectra of hemin solutions displayed overlapping intense bands between 350 and 450 nm with a maximum at 398 nm (Figure 5A, dashed lines) as already observed [33]. The truncated 73aa-Domain was added and, after reaction for 10 min in the absence of oxygen, the sample was gel-filtrated to remove unbound heme. The visible absorption band of hemin sharpened and its maximum shifted to 370 nm (Figure 5A, full line). No increases of the baseline toward shorter wavelengths were apparent excluding any aggregation problem detected at higher concentrations (see above). The hypsochromic shift of the Soret band has been already observed by interaction between heme and a thiolate axial ligand [34, 35].

Similar experiments were carried out with full-length 73aa-Domain. The maximum of the hemin absorption spectrum in the presence of the full-length domain did not shift significantly as compared to free hemin (Figure 5B). This observation is a strong indication that no residues of the 73aa-Domain contribute an axial ligand to heme that would be detected by a change in the electronic properties of the cofactor.

To further evaluate the interaction between heme and the truncated form of the 73aa-Domain, EPR measurements were carried out. The truncated 73aa-Domain was reacted with a 5 fold molar excess of heme, followed by gel filtration (Figure 5C). A low spin ferric iron signal in the $g \sim 2$

region was detected, with g values at 2.45, 2.27 and 1.90. This pattern has already been observed for ferric heme with a thiolate axial ligand [36, 37]. Integration of the signal indicated that only part of the iron present in the sample contributed to the spectrum, suggesting that binding of heme to truncated 73aa-Domain was not quantitative. Alternatively, heme may occur in a mixture of spin-systems contributed by ligation in slightly different modes, as borne out by the observation that, in addition to the low spin signal around $g \sim 2$, a high-spin signal was recorded around $g \sim 6$. Since the sample had been filtrated prior to EPR measurements, it is unlikely that the $g \sim 6$ signal corresponds to unbound heme, and a proportion of heme is probably bound to the sample as a pentacoordinated species contributing a high-spin signal.

The g values of the low spin signal indicate the presence of a weak sixth ligand. These data are similar to those of hexacoordinated heme iron of cytochrome P450 binding to the cysteine of the enzyme active site and to the oxygen atom of a water molecule. There are different from cytochrome P450 experiencing bis-thiolate axial ligation [38]. Our EPR data thus exclude that two truncated domains bind to the heme iron in each axial position. The sixth coordination position of heme bound to the truncated peptide is most probably H_2O or OH^- , since the low spin ferric iron g values shifted from 2.45, 2.27 and 1.90 to 2.36, 2.27 and 1.92 when the pH of the sample was increased from 6.8 to 8.

The EPR spectrum of full-length 73aa-Domain in the presence of hemin was strikingly different from the one of the truncated peptide. A high-spin signal at $g \sim 6$ dominated the spectra (data not shown). Therefore, heme does associate with the full-length peptide since it is not separated by gel filtration, but this interaction does not display signs of strong axial ligation with specific residues of the peptide. This conclusion agrees with those obtained from the NMR and UV-visible spectra.

Purified IRP2 does not bind to the synthesized heme-agarose resin

In order to discriminate between the full-length 106 kDa and the truncated 80 kDa purified IRP2 (Figure 1C) with respect to heme binding, a heme-agarose resin was synthesized. The efficiency of the heme-agarose resin to bind hemoproteins was probed with purified apomyoglobin. A band of 17 kDa corresponding to apomyoglobin interacted with the heme containing resin, but not with non derivatized agarose (Figure 6A).

The purified mix of truncated and full-length IRP2 (Figure 1C) was reacted with the heme-agarose resin to determine whether any of them bound heme. Neither the 106 kDa band, corresponding to full-length IRP2, nor the 80 kDa band, corresponding to the truncated forms of the protein (see above), interacted with the heme agarose resin (Figure 6B). The same experiment was not carried out with the 73aa-Domain since all studied molecular forms of this peptide were found above in NMR and EPR experiments to interact with heme in different ways, and no useful information was expected from such studies.

EPR analyses reveal that purified IRP2 does not provide an axial ligand to heme

The EPR spectra of purified IRP2 and hemin showed a high-spin signal at $g \sim 6$ that was quite similar to the one observed with full-length 73aa-Domain. No low-spin ferric signal was detected. Therefore EPR measurements of purified IRP2, containing the cleaved products of ca. 80 kDa (Figure 1C), did not show any interaction with heme similar to that characterized with truncated 73aa-Domain (Figure 5C). The heme-agarose resin experiment (Figure 6), together with EPR results, showed no specific interactions between heme and purified IRP2, as it was concluded for full-length 73aa-Domain. From these analyses it appears that purified IRP2 does not provide a specific axial ligand to the cofactor, although weak non-specific binding cannot be excluded by our experiments.

DISCUSSION

Production in *E. coli* and purification of IRP2 73aa-Domain afforded several versions of the peptide: the expected full-length domain and truncated forms lacking N-terminal amino acids including most of the lysines, but retaining all cysteines (Figure 1A). The potential interactions of these peptides with heme were studied with a series of complementary methods.

^1H -NMR spectra did not provide any evidence that full-length 73aa-Domain or its truncated ~45-50 amino acids forms are folded. The presence of the N-terminal amino acids of the 73aa-Domain in the full-length form did not trigger the building of secondary structure elements or the occurrence of long range interactions between parts of the domain. Moreover, the addition of iron and zinc salts, or heme did not promote folding of the peptide, whether intact or truncated. However, heme addition to the 73aa-Domain shifted some proton signals. Evidence for interaction between heme and the truncated peptide was provided by the ca. 25 nm hypsochromic shift of the heme Soret band and by the appearance and the characteristics of a low-spin ferric

EPR heme signal. Contrary to globins or cytochromes that provide non-cysteine axial ligands and induce a bathochromic shift of the Soret band of free hemin, the shift observed in our experiments with the truncated peptide, but not with the full-length domain, agrees with cysteine axial ligation to ferric heme. Such cysteine may be contributed by the Heme Regulatory Motif-like sequence (-CPFH-) of the peptide [34, 35, 39]. These data are in agreement with results of TOCSY experiments. Whereas heme interaction with full-length 73aa-Domain obscured some spin systems, probably through relaxation effects, ligation of heme by truncated 73aa-Domain selectively shifted a subset of signals including a set assigned to one of the two phenylalanines. The latter may belong to the Heme Regulatory Motif-like sequence (Cys-Pro-Phe-His) close to the C-terminus of the 73aa-Domain. It is also important to point out that heme binding to this specific site of truncated 73aa-Domain has never been quantitative, i.e. a fraction of our peptide preparations never specifically interacted with heme as deduced from EPR and $^1\text{H-NMR}$ results.

The different heme-binding properties of truncated and full-length 73aa-Domain may be related to different accessibilities of the potential heme-binding site. $^1\text{H-NMR}$ results showed that none of the peptide forms fold under any of the implemented conditions. Therefore both of them are most probably subject to extensive conformational dynamics with a few favored conformations, as deduced from the several $^1\text{H-NMR}$ signatures assigned to the same amino acid (Figure 4). The relatively large size of the full-length peptide may not then stabilize axial coordination to heme. This interpretation is not limited to the situation with isolated peptides since recombinant IRP2 also failed to bind heme immobilized on cross-linked agarose (Figure 6) and to produce a low spin EPR signal with the cofactor. It is noteworthy that not all sequences containing a potential HRM have the ability to bind heme, as shown for the C-terminal portion of the heme-regulated α -subunit of eukaryotic initiation factor-2 kinase [40].

Collectively, the $^1\text{H-NMR}$, EPR and UV-visible absorption results demonstrate a different behavior of truncated and full-length 73aa-Domain towards heme. Clear evidence was obtained indicating a specific, but probably not quantitative, interaction between heme and a cysteine of the truncated peptides, possibly Cys²⁰¹ of the Cys-Pro-Phe-His motif. In contrast, full-length 73aa-Domain does not provide specific ligands to heme, in apparent contradiction with previous conclusions [16-19]. Yamanaka *et al* [17] showed that the absorption spectrum of heme incubated with purified His-tagged IRP2 had a maximum at 420 nm; this result was used as evidence for heme binding to IRP2, but later dismissed as contributed by the His-tag [19]. Jeong

et al [18] reported that the absorption spectrum of a peptide from the specific IRP2 domain showed two maxima upon incubation with heme, at 370 and 420 nm. The material used in this work was a ~63 amino acids peptide spanning the first residue encoded by exon 5 of the human IRP2 gene up to Leu²⁰⁰. Thus, this peptide did not contain the Cys-Pro-Phe-His fragment of the Heme Regulatory Motif-like sequence from Cys²⁰¹ to His²⁰⁴, but it had the other three cysteines (Figure 1A). The modified form in which all these cysteines were replaced by alanines still showed two major peaks at 370 and 420 nm with heme, but of lower intensity than for the wild-type peptide. This would indicate that the peptide still binds heme in the absence of all cysteine residues, otherwise the spectrum should be blank in the visible region (Figure 5, dotted spectra). Instead of showing that one of the three cysteines of the peptide is a heme binding site [18], these results are rather indicative of weak interactions between heme and the 63 amino acids peptide, the specificity of which remains to be established.

The interaction between untagged purified IRP2 and heme has been previously addressed [19]. The maximum of the absorption spectrum was found at 370 nm, as determined here with truncated 73aa-Domain. This preparation was devoid of His-tag, a potential interaction site with heme. The same spectrum also showed a shoulder at 420 nm, as for the bacterial protein Irr [34]. This shoulder is said to indicate a second heme binding site [34], without any further details. It was concluded that IRP2 degradation is triggered by heme binding [19], but the material used in these experiments was not thoroughly characterized for possible proteolysis. It is thus difficult to reconcile these findings with our data. Yet it is now clear that IRP2 proteolysis close to the lysine residues of the 73aa-Domain is a very efficient process that must be taken into account in any studies addressing the turnover mechanism of this protein.

In the present report both full-length and truncated 73aa-Domain peptides contain the exact number of cysteines encoded by exon 5 of the IRP2 gene, and the sequences were confirmed prior to analysis. Our data indicate that intact 73aa-Domain of IRP2 does not display signs of site-specific axial binding to heme. Importantly, even though the isolated truncated form of IRP2 73aa-Domain can bind heme *in vitro*, we evidenced that purified untagged IRP2 does not bind heme immobilized on cross-linked agarose. It may thus be suspected that heme-binding to truncated 73aa-Domain has little biological meaning and that heme interaction with IRP2 is an experimental artefact.

The data in Figure 2A show that, as concluded from *in vitro* experiments, IRP2 is readily cleaved in mammalian cells, presumably near the lysine residues of the 73aa-Domain, to yield a relatively stable intermediate. A cleavage product originating from truncation in the 73aa-Domain has already been reported in rat liver extracts, with the IENTPVL... N-terminal sequence [31]. This cleavage occurs very close to the N-side of the HRM-like sequence. It is different from the fragment characterized herein, but *i*) different biological materials were used in both studies, *ii*) the Ser-Ser-Gln[Ile-Glu-Asn cleavage site is not one of a conventional endoprotease, and *iii*) the Ile-Glu-Asn ... starting sequence may result from exoproteolytic processing of a longer product. In both the previous [31] and the present studies (Figure 2), cleavage occurs in the 73aa-Domain and it is iron-independent. The ca. 80 kDa C-terminal end of IRP2 does not bind to heme agarose (Figure 6). Altogether these results do not support a function for this degradation intermediate as an efficient heme sensor *in vivo*. Nevertheless, the demonstration of the occurrence of this intermediate reveals an as yet unsuspected mechanistic hint of IRP2 degradation, in which endoproteases cleave the protein at closely-spaced specific sites located within the 73aa-Domain.

The results presented herein indicate that IRP2 may be degraded in cells by additional pathways to the one leading to the proteasome [14, 41-43]. The mechanism by which this protein senses intracellular iron awaits further investigation. It is conceivable that intracellular iron or heme levels may control IRP2 abundance in an indirect manner, possibly involving iron- or heme-dependent properties of accessory partners.

ACKNOWLEDGMENTS:

The contribution of Laura Udakis to some of the reported experiments is acknowledged. Dr Cécile Bouton is thanked for the gift of the anti-IRP2 antibody. This work was supported by a travel grant for Camille Dycke from Centre Jacques Cartier (Lyon, France).

REFERENCES

- 1 Hentze, M. W., Muckenthaler, M. U. and Andrews, N. C. (2004) Balancing acts: molecular control of mammalian iron metabolism. *Cell* **117**, 285-97
- 2 Wallander, M. L., Leibold, E. A. and Eisenstein, R. S. (2006) Molecular control of vertebrate iron homeostasis by iron regulatory proteins. *Biochim. Biophys. Acta* **1763**, 668-89
- 3 Wingert, R. A., Galloway, J. L., Barut, B., Foott, H., Fraenkel, P., Axe, J. L., Weber, G. J., Dooley, K., Davidson, A. J., Schmid, B., Paw, B. H., Shaw, G. C., Kingsley, P., Palis, J., Schubert, H., Chen, O., Kaplan, J. and Zon, L. I. (2005) Deficiency of glutaredoxin 5 reveals Fe-S clusters are required for vertebrate haem synthesis. *Nature* **436**, 1035-39
- 4 Sposi, N. M., Cianetti, L., Tritarelli, E., Pelosi, E., Miliati, S., Barberi, T., Gabbianelli, M., Saulle, E., Kühn, L., Peschle, C. and Testa, U. (2000) Mechanisms of differential transferrin receptor expression in normal hematopoiesis. *Eur. J. Biochem.* **267**, 6762-74
- 5 Schranzhofer, M., Schiffrer, M., Cabrera, J. A., Kopp, S., Chiba, P., Beug, H. and Müllner, E. W. (2006) Remodeling the regulation of iron metabolism during erythroid differentiation to ensure efficient heme biosynthesis. *Blood* **107**, 4159-67
- 6 LaVaute, T., Smith, S., Cooperman, S., Iwai, K., Land, W., Meyron-Holtz, E., Drake, S. K., Miller, G., Abu-Asab, M., Tsokos, M., Switzer, R., 3rd, Grinberg, A., Love, P., Tresser, N. and Rouault, T. A. (2001) Targeted deletion of the gene encoding iron regulatory protein-2 causes misregulation of iron metabolism and neurodegenerative disease in mice. *Nat. Genet.* **27**, 209-14
- 7 Cooperman, S. S., Meyron-Holtz, E. G., Olivierre-Wilson, H., Ghosh, M. C., McConnell, J. P. and Rouault, T. A. (2005) Microcytic anemia, erythropoietic protoporphyria, and neurodegeneration in mice with targeted deletion of iron-regulatory protein 2. *Blood* **106**, 1084-91
- 8 Galy, B., Ferring, D., Minana, B., Bell, O., Janser, H. G., Muckenthaler, M., Schumann, K. and Hentze, M. W. (2005) Altered body iron distribution and microcytosis in mice deficient in iron regulatory protein 2 (IRP2). *Blood* **106**, 2580-9
- 9 Smith, S. R., Ghosh, M. C., Olivierre-Wilson, H., Hang Tong, W. and Rouault, T. A. (2006) Complete loss of iron regulatory proteins 1 and 2 prevents viability of murine zygotes beyond the blastocyst stage of embryonic development. *Blood Cells Mol. Dis.* **36**,

- 283-7
- 10 Galy, B., Holter, S. M., Klopstock, T., Ferring, D., Becker, L., Kaden, S., Wurst, W., Grone, H. J. and Hentze, M. W. (2006) Iron homeostasis in the brain: complete iron regulatory protein 2 deficiency without symptomatic neurodegeneration in the mouse. *Nat. Genet.* **38**, 967-9; discussion 969-70
 - 11 Meyron-Holtz, E. G., Ghosh, M. C. and Rouault, T. A. (2004) Mammalian tissue oxygen levels modulate iron-regulatory protein activities in vivo. *Science* **306**, 2087-90
 - 12 Meyron-Holtz, E. G., Ghosh, M. C., Iwai, K., LaVaute, T., Brazzolotto, X., Berger, U. V., Land, W., Ollivierre-Wilson, H., Grinberg, A., Love, P. and Rouault, T. A. (2004) Genetic ablations of iron regulatory proteins 1 and 2 reveal why iron regulatory protein 2 dominates iron homeostasis. *EMBO J.* **23**, 386-95
 - 13 Samaniego, F., Chin, J., Iwai, K., Rouault, T. A. and Klausner, R. D. (1994) Molecular Characterization of a Second-Responsive Element Binding Protein, Iron regulatory Protein 2. Structure, Function and Post-Transcriptional Regulation. *J. Biol. Chem.* **269**, 30904-30910
 - 14 Iwai, K., Klausner, R. D. and Rouault, T. A. (1995) Requirements for iron-regulated degradation of the RNA binding protein, iron regulatory protein 2. *EMBO J.* **14**, 5350-7
 - 15 Iwai, K., Drake, S. K., Wehr, N. B., Weissman, A. M., LaVaute, T., Minato, N., Klausner, R. D., Levine, R. L. and Rouault, T. A. (1998) Iron-dependent oxidation, ubiquitination, and degradation of iron regulatory protein 2: implications for degradation of oxidized proteins. *Proc. Natl. Acad. Sci. U S A* **95**, 4924-8
 - 16 Kang, D. K., Jeong, J., Drake, S. K., Wehr, N. B., Rouault, T. A. and Levine, R. L. (2003) Iron Regulatory Protein 2 as Iron Sensor. Iron-dependent oxidative modification of cysteine. *J. Biol. Chem.* **278**, 14857-64
 - 17 Yamanaka, K., Ishikawa, H., Megumi, Y., Tokunaga, F., Kanie, M., Rouault, T. A., Morishima, I., Minato, N., Ishimori, K. and Iwai, K. (2003) Identification of the ubiquitin-protein ligase that recognizes oxidized IRP2. *Nat. Cell. Biol.* **5**, 336-40
 - 18 Jeong, J., Rouault, T. A. and Levine, R. L. (2004) Identification of a heme-sensing domain in iron regulatory protein 2. *J. Biol. Chem.* **279**, 45450-4
 - 19 Ishikawa, H., Kato, M., Hori, H., Ishimori, K., Kirisako, T., Tokunaga, F. and Iwai, K. (2005) Involvement of heme regulatory motif in heme-mediated ubiquitination and

- degradation of IRP2. *Mol. Cell* **19**, 171-81
- 20 Hanson, E. S., Rawlins, M. L. and Leibold, E. A. (2003) Oxygen and iron regulation of iron regulatory protein 2. *J. Biol. Chem.* **278**, 40337-42
- 21 Wang, J., Chen, G., Muckenthaler, M., Galy, B., Hentze, M. W. and Pantopoulos, K. (2004) Iron-mediated degradation of IRP2, an unexpected pathway involving a 2-oxoglutarate-dependent oxygenase activity. *Mol. Cell. Biol.* **24**, 954-65
- 22 Tabor, S. (1990) in *Current Protocols in Molecular Biology* (Ausubel, F. A., Brent, R., Kingston, R. E., Moore, D. D., Seidman, J. G., Smith, J. A. and Struhl, K., eds.), pp. 16.2.1-16.2.11, Greene Publishing and Wiley-Interscience, New York
- 23 Martelli, A. and Moulis, J.-M. (2004) Zinc and cadmium specifically interfere with RNA-binding activity of human iron regulatory protein 1. *J. Inorg. Biochem.* **98**, 1413-20
- 24 Wang, J. and Pantopoulos, K. (2002) Conditional derepression of ferritin synthesis in cells expressing a constitutive IRP1 mutant. *Mol. Cell. Biol.* **22**, 4638-51
- 25 Piotto, M., Saudek, V. and Sklenar, V. (1992) Gradient-Tailored Excitation for Single-Quantum Nmr-Spectroscopy of Aqueous-Solutions. *J. Biomol. NMR* **2**, 661-665
- 26 Hwang, T. L. and Shaka, A. J. (1995) Water Suppression That Works - Excitation Sculpting Using Arbitrary Wave-Forms and Pulsed-Field Gradients. *J. Magn. Reson. Series A* **112**, 275-279
- 27 Schanda, P., Forge, V. and Brutscher, B. (2006) HET-SOFAST NMR for fast detection of structural compactness and heterogeneity along polypeptide chains. *Magn. Reson. Chem.* **44**, S177-S184
- 28 Brazzolotto, X., Gaillard, J., Pantopoulos, K., Hentze, M. W. and Moulis, J.-M. (1999) Human cytoplasmic aconitase (Iron regulatory protein 1) is converted into its [3Fe-4S] form by hydrogen peroxide in vitro but is not activated for iron-responsive element binding. *J. Biol. Chem.* **274**, 21625-30
- 29 Martelli, A., Salin, B., Dycke, C., Louwagie, M., Andrieu, J.-P., Richaud, P. and Moulis, J.-M. (2007) Folding and turnover of human iron regulatory protein 1 depend on its subcellular localization. *FEBS J.* **274**, 1083-92
- 30 Dupuy, J., Volbeda, A., Carpentier, P., Darnault, C., Moulis, J.-M. and Fontecilla-Camps, J. C. (2006) Crystal structure of human iron regulatory protein 1 as cytosolic aconitase. *Structure* **14**, 129-39

- 31 Guo, B., Yu, Y. and Leibold, E. A. (1994) Iron regulates cytoplasmic levels of a novel iron-responsive element-binding protein without aconitase activity. *J. Biol. Chem.* **269**, 24252-60
- 32 Goessling, L. S., Mascotti, D. P. and Thach, R. E. (1998) Involvement of heme in the degradation of iron-regulatory protein 2. *J. Biol. Chem.* **273**, 12555-7
- 33 de Villiers, K. A., Kaschula, C. H., Egan, T. J. and Marques, H. M. (2007) Speciation and structure of ferriprotoporphyrin IX in aqueous solution: spectroscopic and diffusion measurements demonstrate dimerization, but not mu-oxo dimer formation. *J. Biol. Inorg. Chem.* **12**, 101-17
- 34 Qi, Z., Hamza, I. and O'Brian, M. R. (1999) Heme is an effector molecule for iron-dependent degradation of the bacterial iron response regulator (Irr) protein. *Proc. Natl. Acad. Sci. U S A* **96**, 13056-61
- 35 Suzuki, H., Tashiro, S., Hira, S., Sun, J., Yamazaki, C., Zenke, Y., Ikeda-Saito, M., Yoshida, M. and Igarashi, K. (2004) Heme regulates gene expression by triggering Crm1-dependent nuclear export of Bach1. *EMBO J.* **23**, 2544-53
- 36 Dawson, J. H., Andersson, L. A. and Sono, M. (1983) The diverse spectroscopic properties of ferrous cytochrome P-450-CAM ligand complexes. *J. Biol. Chem.* **258**, 13637-45
- 37 Stuehr, D. J. and Ikeda-Saito, M. (1992) Spectral characterization of brain and macrophage nitric oxide synthases. Cytochrome P-450-like hemeproteins that contain a flavin semiquinone radical. *J. Biol. Chem.* **267**, 20547-50
- 38 Sono, M. and Dawson, J. H. (1982) Formation of low spin complexes of ferric cytochrome P-450-CAM with anionic ligands. Spin state and ligand affinity comparison to myoglobin. *J. Biol. Chem.* **257**, 5496-502
- 39 Zhang, L. and Guarente, L. (1995) Heme binds to a short sequence that serves a regulatory function in diverse proteins. *EMBO J.* **14**, 313-20
- 40 Rafie-Kolpin, M., Chefalo, P. J., Hussain, Z., Hahn, J., Uma, S., Matts, R. L. and Chen, J. J. (2000) Two heme-binding domains of heme-regulated eukaryotic initiation factor-2alpha kinase. N terminus and kinase insertion. *J. Biol. Chem.* **275**, 5171-8
- 41 Guo, B., Phillips, J. D., Yu, Y. and Leibold, E. A. (1995) Iron regulates the intracellular degradation of iron regulatory protein 2 by the proteasome. *J. Biol. Chem.* **270**, 21645-51

- 42 Kim, S., Wing, S. S. and Ponka, P. (2004) S-nitrosylation of IRP2 regulates its stability
via the ubiquitin-proteasome pathway. *Mol. Cell. Biol.* **24**, 330-7
- 43 Wang, J. and Pantopoulos, K. (2005) The pathway for IRP2 degradation involving 2-
oxoglutarate-dependent oxygenase(s) does not require the E3 ubiquitin ligase activity of
pVHL. *Biochim. Biophys. Acta* **1743**, 79-85

FIGURES LEGENDS

Figure 1: Cleavage of purified 73aa-Domain and IRP2.

(A) N-terminal sequencing of the purified 73aa-Domain of IRP2 reveals the presence of truncated products. The 73aa-Domain sequence is indicated on the first line. The underlined amino acids at the N- and C-termini are those encoded across the splice junctions and the first cysteine does not belong to the construction used. The phenylalanines discussed in the text are starred, the cysteines are squared, and the HRM-like sequence is boxed. The N-termini of other detected products are shown on the other lines, with their respective proportions. (B) Electrophoretic Mobility Shift-Assay of purified recombinant IRP2. 1: labeled IRE probe alone; 2: recombinant IRP2 incubated with an excess of IRE probe. Two wells from the same gel were put side by side for the Figure. (C) Two major bands were obtained after the last step of recombinant IRP2 purification. Active fractions from each purification step, 1: crude extract; 2: DE52; 3: Phenyl Sepharose; 4: Superdex; 5: heparin-affinity, were separated on 8% SDS-PAGE and stained with Coomassie blue. The left lane displays molecular weight markers.

Figure 2: Cleavage of IRP2 in H1299 cells.

(A) IRP2-HA turnover in H1299 cells. After induction for 48 hr, tetracycline was added back to cells for different times, indicated in hours below each lane. The tet⁺ label corresponds to extracts of control cells kept in the presence of tetracycline, i.e. without induction of IRP2-HA cDNA expression. Fifty µg of total cell lysates were analyzed by SDS-PAGE on 8% gels. Western blots were probed using anti-HA (upper part) or anti-β-actin (lower part) antibodies on two pieces of the membrane. In some cases, only a few wells of the same gel are presented, as these gels contained more samples than needed for the considered Figure. (B) IRP2-HA specific cleavage is iron-independent. After induction for 48 hr, tetracycline was added back to cells for 4 hr (lane -), with 50 µg/ml of iron ammonium citrate (FAC) or with 100 µM desferrioxamine (DFO). Fifty µg of total cell lysates were analyzed as in (A). The second faint band above the ca. 80kDa product is non specific as it can be seen in the tet⁺ (uninduced) well in the absence of IRP2-HA. (C) IRP2_{Δ73}-HA is not specifically cleaved in H1299 cells. After 48 hr-induction of IRP2_{Δ73}-HA by removal of tetracycline, cells were put back in the tetracycline-containing medium for 0, 2, 4, 8, or 24 hr and analyzed as above.

Figure 3: ^1H -watergate spectra of the 73aa-Domain.

Spectra were recorded for the truncated peptide (**A**), full-length 73aa-Domain (**B**), the truncated peptide in the presence of ZnCl_2 (**C**), of FeSO_4 (**D**), or hemin (**E**), and for the full-length peptide in the presence of hemin (**F**). Peaks labeled with * have been identified as non exchangeable protons on spectra recorded in D_2O and are considered in the TOCSY spectra discussed in the text. In (**F**) s stands for peaks of residual DMF used to dissolve the added hemin. The intensity of the signals in the amide region on the left is multiplied by ten as compared to that in the aliphatic region on the right.

Figure 4: Analysis of heme-binding on full-length and truncated 73aa-Domain peptides through 2D TOCSY experiments.

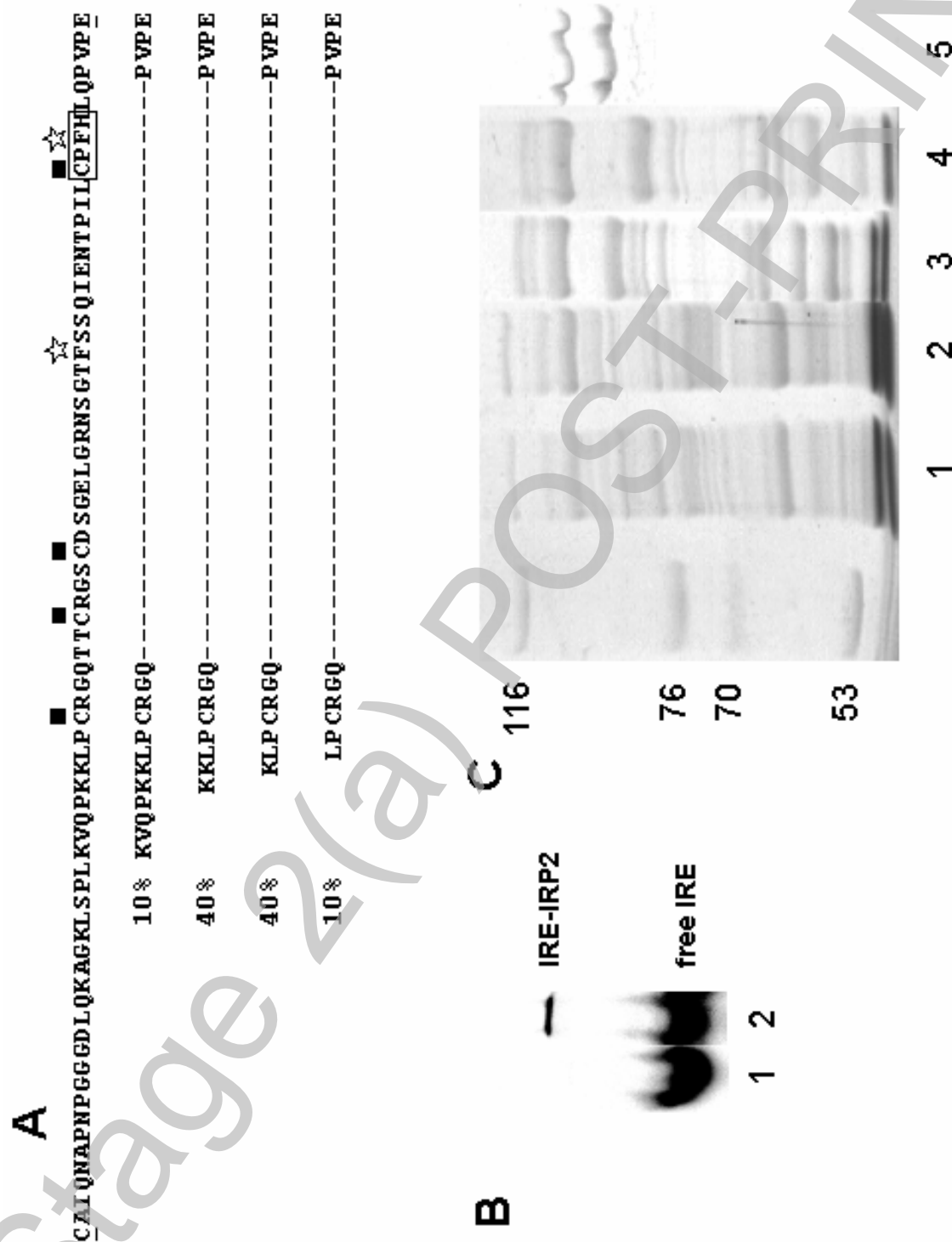
Aromatic region of the TOCSY spectra collected with extensive water suppression and with 70 ms mixing time on truncated (**A**) and full-length (**B**) 73aa-Domain peptide. Samples in 50 mM phosphate buffer in $\text{H}_2\text{O}:\text{D}_2\text{O}$ 90:10 (v:v) at pH 7 were reacted with hemin as described in Experimental. Corresponding 1D spectra collected with the same water suppression scheme on the truncated and full-length peptide samples are reported in (**C**) and (**D**), respectively. Circles emphasize differences between the two 2D-spectra. The two phenylalanines found in both truncated (a) and full-length (b) 73aa-Domain are arbitrarily labeled with subscripts 1 and 2. As they occur in different local conformations, the corresponding spin-systems are labeled i, ii, and iii (see Supplementary data). The correlations are drawn with dashed lines. Additional unassigned spin-systems are labeled with subscripts 4, 5, and 6.

Figure 5: Interaction of heme with the IRP2 73aa-Domain studied by absorption spectroscopy and EPR.

(**A**) Absorption spectra of the truncated peptide in 50 mM phosphate buffer, 0.25 M NaCl, pH 8 in the absence (dotted line) and in the presence of one equivalent of heme (continuous line). The hemin absorption spectrum is shown for reference (discontinuous line). (**B**) Absorption spectra of the intact peptide with symbols as in (**A**). Maxima for the heme-peptide complexes are indicated. (**C**) EPR spectrum in the $g \sim 2$ region of the complex between heme and the truncated form of IRP2 73aa-Domain. Microwave frequency 9.655 GHz; microwave power 4 mW; receiver gain 4×10^5 ; modulation amplitude 1 mT, temperature 13 K.

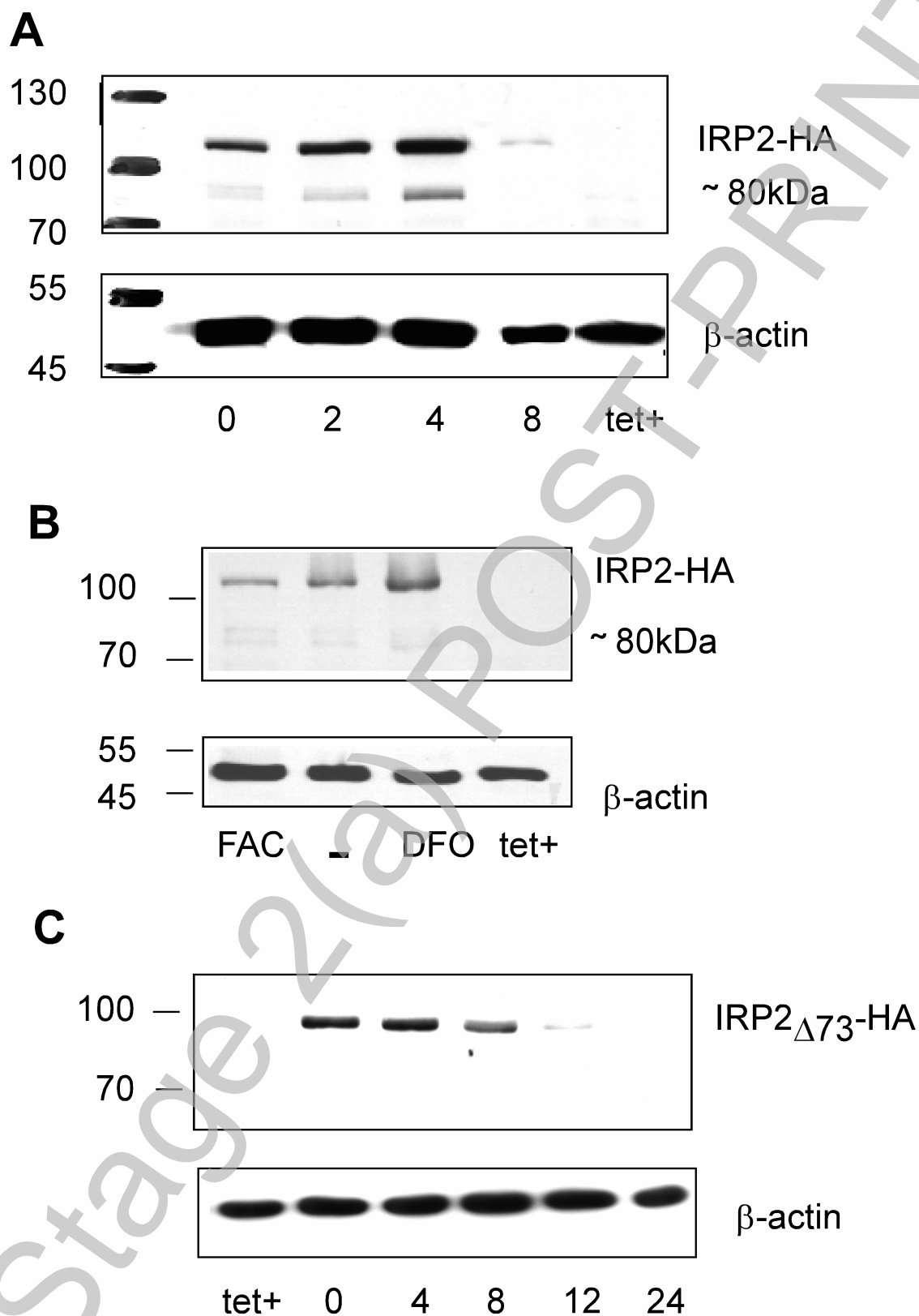
Figure 6: Apomyoglobin binds to heme agarose resin whereas purified IRP2 does not.

(A) interaction between purified apomyoglobin and the heme-agarose resin or non derivatized agarose resin. Fractions were analyzed by SDS-PAGE on a 12% gel, followed by silver nitrate staining. The loaded fractions were: heme-agarose resin pass-through after loading (PT), purified apomyoglobin as a control (myo), apomyoglobin eluted from the heme resin agarose with 8M urea (E), and control sample eluted after washing from the interaction between the non-derivatized agarose resin and apomyoglobin (C). (B) Interaction between purified IRP2 and the heme-agarose affinity resin: pass-through fraction (PT), first rinse with washing buffer (W), and material eluted using 8 M urea (E).

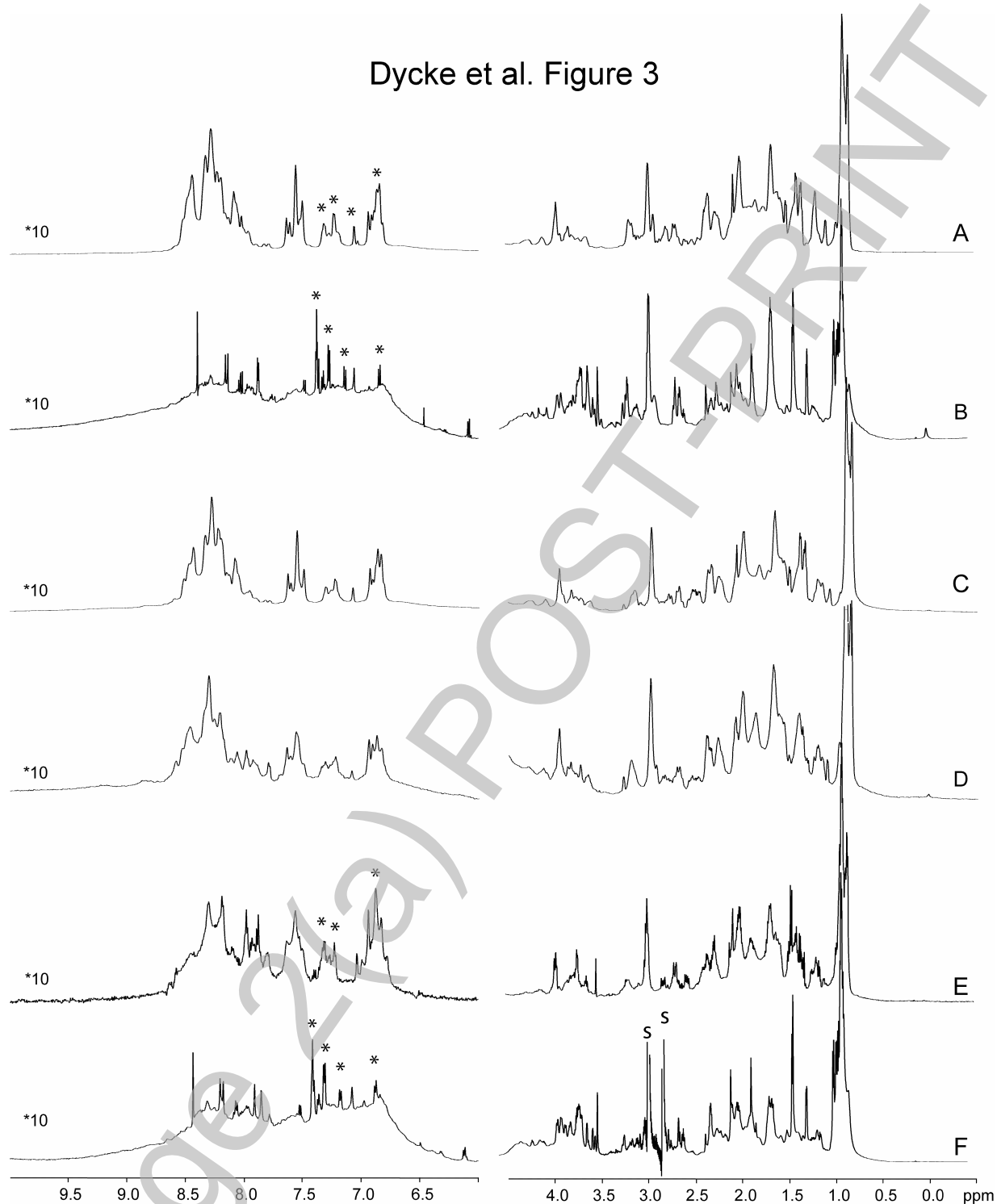


Dycke et al. Figure 1

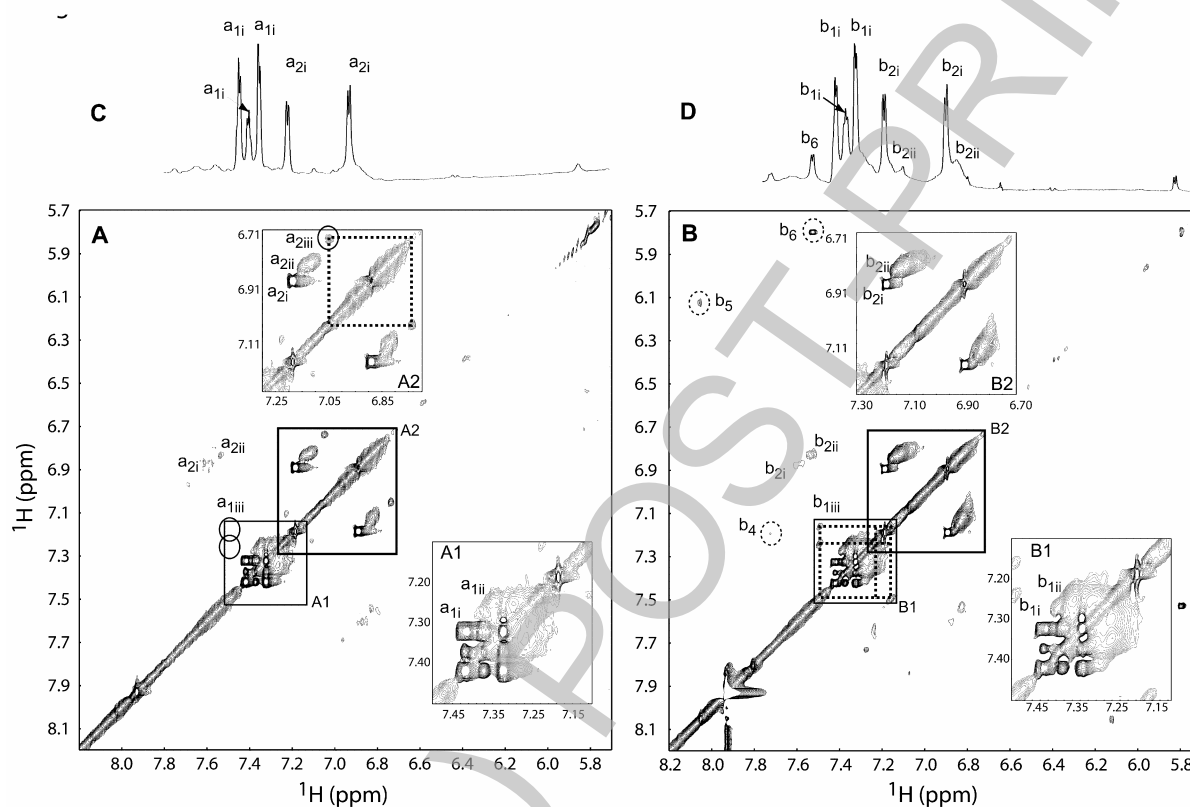
Dycke et al. Figure 2



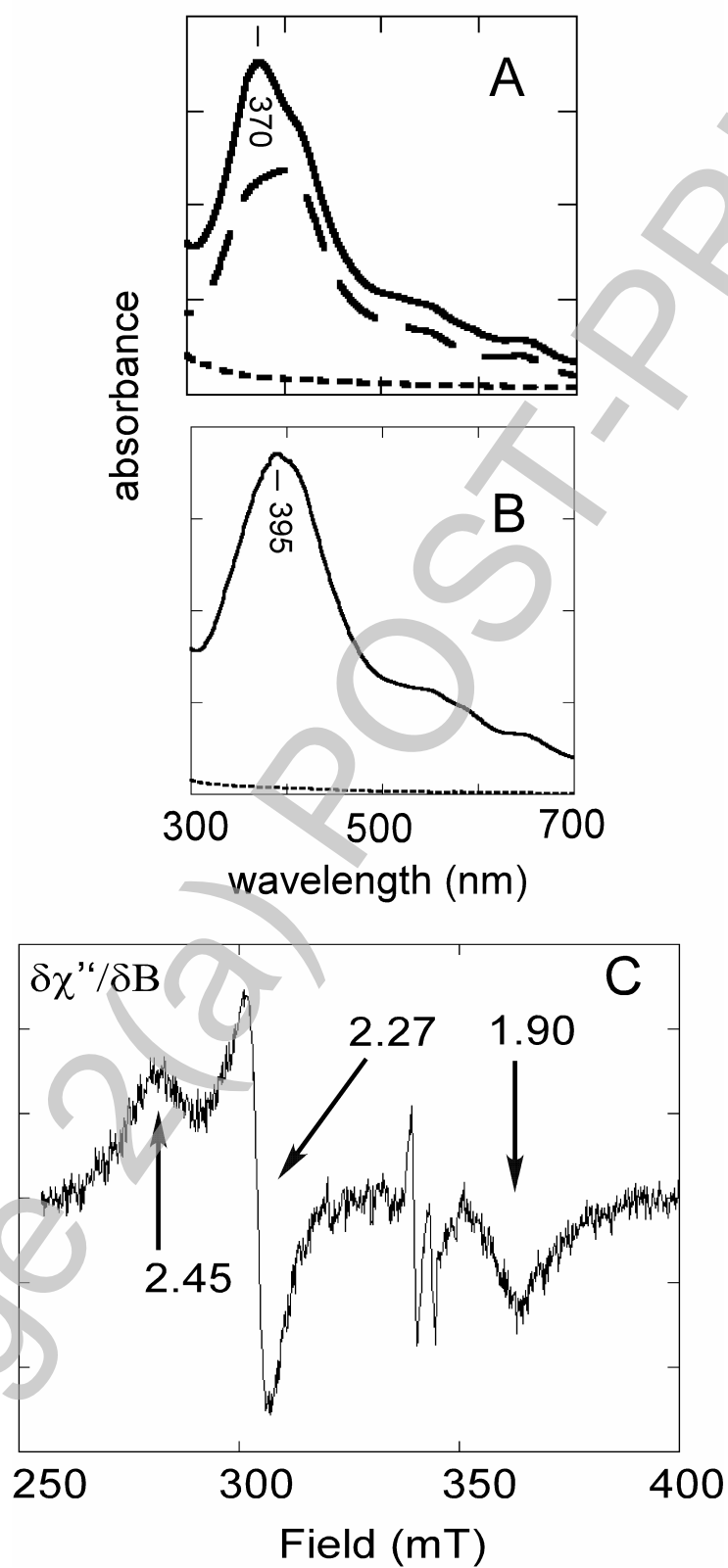
Dycke et al. Figure 3



Dycke et al. Figure 4



Dycke et al. Figure 5



Dycke et al. Figure 6

